

# Rational Thickness Design of an Airport Runway for Boeing 777 Aircraft Loading

D.V. RAMSAMOOJ\*

*Professor of Civil Engineering, California State University, Fullerton, 800 N. State College Blvd., Fullerton, CA 92634, USA*

*(Received April 03, 1999; Revised January 28, 2000)*

A rational method of design for the thickness of concrete runways and taxiways against the fatigue mode of distress is presented. The material properties used for design are the tensile strength, the fracture toughness, the Young's modulus, Poisson's ratio and the lower threshold stress intensity factor corresponding to the endurance limit. A new method of stress analysis comprising the use of multilayered Elastic theory combined with *Fracture Mechanics (EFM)* is used to determine the stresses in the jointed pavements caused by the gear loads and by thermal curl stress. The effect of the combined thermal and aircraft gear load stresses including the lateral wander of the gear loads is handled rationally. The stresses are then used to compute the fatigue life, using fracture mechanics, for several concrete thicknesses, from which the final design for 500,000 applications of Boeing 777 loading is selected.

*Keywords:* Multilayered elasticity, fracture mechanics, concrete, fatigue, thermal and aircraft stresses

## INTRODUCTION

The present state-of-the art of structural design of concrete runways is mechanistic-empirical, based on observation of full-scale airport pavements. Some design procedures are based on the maximum bending stress in the interior of the pavement generated by the aircraft (Packard, 1973). The width between the center of the gear loads for a Boeing 777 aircraft (B 777) is 10.97 m. For a runway joint spacing of 7.62 m, the aircraft, *if centered on the runway* with respect to the joints in the PCC, would travel with the edge of the wheel load at a distance of 1.21 m from the nearest longitudinal joint. The actual traffic pattern for a runway at about mid-length has a lateral

wander of  $\pm 9.0$  m as shown in Figure 1(b) (Packard, 1973). From the distribution of the traffic, approximately 7.5% of the gear loads fall in the vicinity of the longitudinal joint, so that the bending stresses are considerably greater than those at the interior.

The Federal Aviation Agency (FAA) (FAA Advisory Circular AC 150-5320-6C) uses 75% of the Westergaard *edge bending stress* as the design stress, obtaining a more realistic design stress than that at the interior. This was obtained by correlating the linear elastic interior stress with the Westergaard edge stresses for different aircraft types and subgrade strengths. However, the decision to use a single value of the equivalent stress for design purposes should be based on rational performance criteria, such as fatigue

\* Corresponding author: Tel: (714) 278-3968, FAX: (714) 278 3916, e-mail: dramsamooj@fullerton.edu



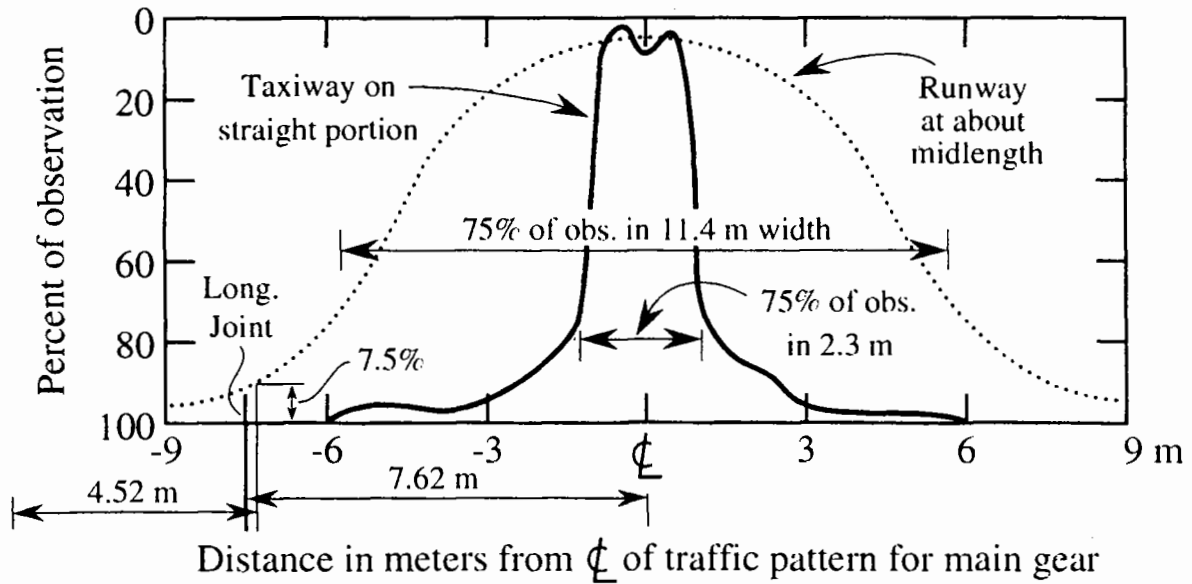


FIGURE 1(b). Traffic Distribution Patterns for Dual and Dual-Tandem Gear Aircraft

newer materials more efficiently and economically. Today, in the greatest age of technology, rational methods, validated by experimental laboratory and field data, are quite feasible. Such a design method is presented below. The notation used is summarised in the Appendix.

**CRACK INITIATION AND PROPAGATION IN CONCRETE PAVEMENTS**

The existence of crack-like flaws, whether arising from initial defects in the material, from fabrication or from service conditions, cannot be precluded from any engineering structure. Cracks initiate from these starter defects and the rate of crack propagation is best described by fracture mechanics. (Ramsamooj, 1994a).

Concrete (PCC) contains numerous flaws, such as holes or air pockets, precracked aggregates, lack of bond between aggregate and matrix, etc., that are sufficiently large, from which cracking may originate after the first loading cycle. The size of the inherent

defect or starter crack is equal to (Ouchterlony, 1983, Ramsamooj, 1994a)

$$c_0 = 0.05(K_{Ic}/f_r)^2 \tag{1}$$

where  $K_{Ic}$  is the plane strain fracture toughness and  $f_r$  is the modulus of rupture. For flexural fatigue of a concrete pavement, it is assumed that the maximum stress occurs at the bottom edge at the longitudinal joint, midway between the transverse joints. The starter crack is initiated here and it is assumed to be quarter-elliptical with a shape factor of  $a/c = 0.5$ . Under repeated loading the crack will grow in the transverse plane in all directions. When the leading edge of the vertical crack-front passes about five-eighths of the thickness of the concrete slab, crack propagation becomes very rapid and break-through occurs. From this point, the crack then propagates as a through-crack with the top slightly smaller than the bottom. Thus, crack propagation a concrete pavement has two distinct stages; firstly as a quarter-elliptical crack at the bottom of the concrete at the edge midway between the transverse joints and secondly as a through-crack. To evaluate the rate of crack

propagation, the stress intensity factor (SIF) for each type of crack is needed.

### Stress Intensity Factors

#### Quarter-elliptical crack

For a semi-elliptical or quarter-elliptical crack, with minor and major semi-axes  $a$  and  $c$  respectively, the SIFs at the leading vertical and horizontal edges of the crack tip are given by Grandt and Sinclair (1972).

#### Through-crack in a slab on elastic foundation

Consider an infinite plate on an elastic foundation with a through-crack of length  $2c$ . For a constant bending moment over the crack surfaces, Folias (1970) obtained a theoretical solution for the Mode I SIF, given by

$$K_{Iref} = \frac{\sigma\sqrt{c\pi}}{1 + a(\lambda c)^2} \quad (2)$$

where  $c$  is the crack length,  $\sigma$  is the constant bending stress over the crack surface,  $\lambda = \sqrt{k/D}$  is the inverse characteristic length,  $a$  is a constant = 0.125 for  $\lambda c < 3$ . The SIF for any other symmetrical load system may be obtained by the weight function method, (Petroski and Achenbach, (1978) as

$$K_I = \int_0^c (\sigma(x))h(c, x)dx \quad (3)$$

in which  $\sigma(x)$  is the stress distribution across the plane of the crack in the uncracked body, loaded by the force system for which the  $K$  value is being determined,  $x$  is the coordinate distance measured from the center of the crack along the crack, and  $h$  is a weight function given by Ramsamooj (1998) as

$$h = \frac{2(1 - a\lambda^2 c^2 + 2a\lambda^2 x^2)}{1 + a\lambda^2 c^2 \sqrt{c\pi(1 - (x/c)^2)}} \quad (4)$$

The opening Mode I SIF for a specified stress distribution on the crack faces may be obtained from Eq. (4). The integration is done across the plane of the crack in the uncracked body. Various types of loading may be superposed.

The stresses in the jointed pavement are found by a new method called EFM. This method, which combines the Theory of Elasticity with Fracture Mechanics was presented by Ramsamooj (1999). A brief summary of the procedure is as follows.

(1) Elastic theory is used to determine the SIFs for the pavement as an infinite plate on an elastic foundation. The resulting deflection and stresses in the *unjoints or uncracked* slab caused by the gear loads are computed from the multilayered elastic program CHEVRON (Chevron Co. 1978)

(2) Fracture mechanics is used to determine the stresses caused by the joints. The joints are treated like cracks with no interfacial forces, and

(3) The final stresses are obtained by superposition.

By analogy (Sih and Liebowitz, 1968), the stress intensity factor for the tearing Mode III, subject to the restrictions of plane strain or generalized plane stress is:

$$K_{III} = \int_0^c \tau(x)h(c, x)dx \quad (5)$$

in which  $\tau(x)$  is the shear stress on the crack surface. For combined Modes I and III, the equivalent SIF is obtained from the maximum principal stress theory (De-Chang and Zhu, 1982).

### Deflection at point P caused by a load at P due to the joints

From the SIFs, the deflection of the pavement at any point P caused by a load at P is obtained from the relationship that gives the *change in the deflection of the pavement at a point caused by a joint or crack*, for symmetrical loading as (Ramsamooj, 1998)

$$w_P = 4 \int_0^l \frac{K_I^2(1 - \nu^2)H}{PE} dc \quad (6)$$

in which  $H$  is the thickness of the concrete slab,  $P$  is the wheel load,  $E$  and  $\nu$  are the Young's modulus and Poisson's ratio, respectively, and  $l$  is the half-length of the joint.

**Deflection at point Q due to the load at P, due to the joints**

The deflection at any point Q caused by a wheel load in the position P shown in Figure 1, is given by (Ramsamooj, 1998) as

$$w_{QP} = \frac{2(1 - \nu^2)}{P_w E} \int_0^1 (K_{IP} K_{IQ}) H dc \quad (7)$$

in which  $K_{IP}$  and  $K_{IQ}$  are the SIFs for the crack due to the loads at P and at Q, respectively. Therefore the deflection profile of the concrete slab along the crack or along the midnormal to the crack can be found.

**Deflection at a point P caused by the load at Q for combined bending and shear, due to the joints**

A wheel load positioned at a point P along the midnormal to the crack, causes a bending stress as well as a shear stress along the joint. This generates deformation in both Modes I and III. The values of  $K_I$  and  $K_{III}$  are determined from Equations (4) and (5), respectively. The equivalent Mode I SIF for the combined bending and shear stresses for the load at P and Q, respectively, are denoted as  $K_{IeqP}$  and  $K_{IeqQ}$  (De-Chang and Zhu, 1982). The deflection at Q caused by the load P is

$$w_{QP} = \frac{4(1 - \nu^2)}{P_w E} \int_0^1 (K_{IeqP} K_{IeqQ}) H dc \quad (8)$$

Equations (6), (7) and (8) give the change in the deflection caused by the joints at any point on the midnormal to the crack for any position of the load. From the deflection, the stresses generated by the gear loads are calculated from plate theory and superposed on those for the unjointed pavement to obtain the total stresses in the jointed pavement.

**Bending stress with gear load tangent to the longitudinal joint**

The tensile bending stress that is usually used for designing concrete pavements is with the tire contact area of a wheel load tangent to the longitudinal joint. The boundary condition at a joint in the concrete is that the bending stress on the free surface in the

y-direction (Figure 1) is zero. Therefore the stresses caused by the joint must be equal and opposite to those caused by the primary load, so that

$$D \left( \frac{\partial^2 w}{\partial y^2} + \nu \frac{\partial^2 w}{\partial x^2} \right)_c = M_y \quad (9)$$

in which  $M_y$  = bending moment caused by the primary loading, and the suffix, c, refers to the terms caused by the joint. The value of  $\partial^2 w / \partial y^2$  is obtained from Equation (9). The second derivative in the x-direction  $\partial^2 w / \partial x^2$  is obtained from the deflection profile along the edge using finite difference, or

$$\frac{\partial^2 w}{\partial x^2} = 2 \frac{w_2 - w_1}{\Delta x^2} \quad (10)$$

in which  $w_1$  and  $w_2$  are the deflection at the midslab position and at a distance  $\Delta x$  from it. The bending moment in the x-direction at the midslab position is one of the stresses required for design purposes in highway pavements. It is given by

$$M_x = -D \left( \frac{\partial^2 w}{\partial x^2} + \nu \frac{\partial^2 w}{\partial y^2} \right) \quad (11)$$

For more details of the stress analysis, the interested reader is referred to Ramsamooj (1999). The calculations for the stresses are done by a computer program called CONPAVE.

**FATIGUE CRACK PROPAGATION**

Clemmer (1922) determined the endurance or fatigue limit to be 51–54% of the static flexural strength for plain concrete subjected to stresses ranging from zero to maximum in tension. Kesler (1953) found no fatigue limit within 10 million stress repetitions at a stress of 62% of the static ultimate flexural strength. In his review of the fatigue of concrete, Nordby (1958) concluded that the endurance limit was about 50–55% of the static ultimate flexural stress; his exact statement was that “all investigators are in substantial agreement with this.” Nordby's statement is not a contradiction of the findings of Kesler; since the endurance limit theoretically corresponds to an infinite number of cycles of loading. Accordingly, the endurance limit in this paper is assumed to be 52.5% of the

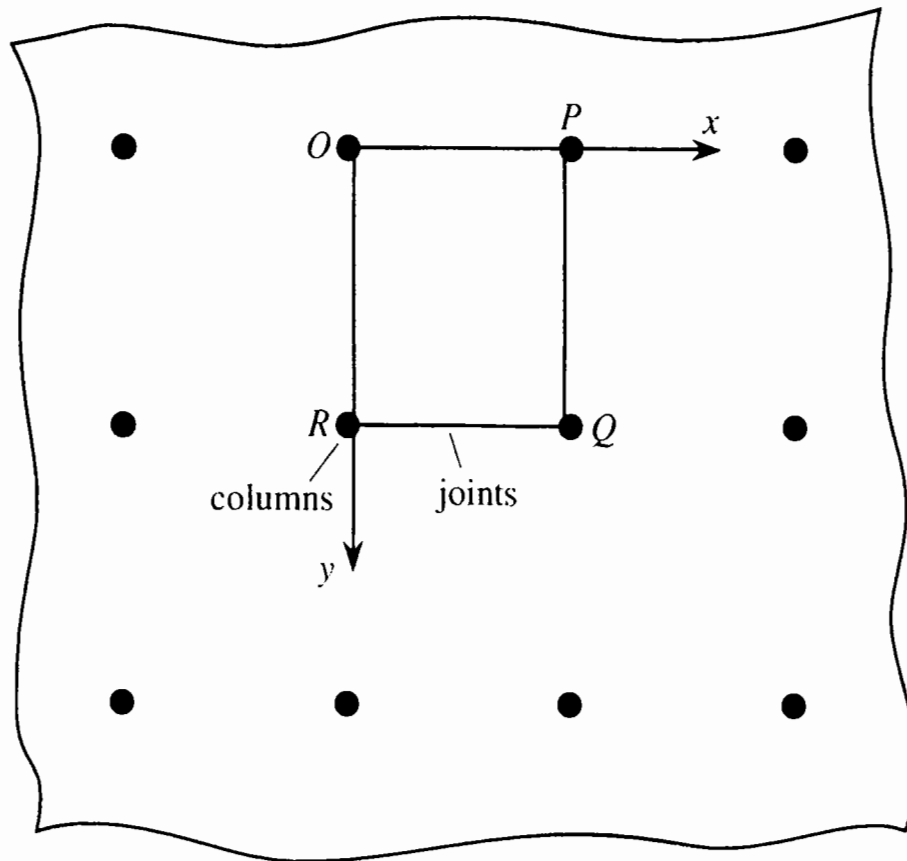


FIGURE 2 Flat Slab with Joints along Column Lines forming a Slab Supported at the Corners

modulus of rupture. The endurance limit is related to the threshold SIF by

$$K_0 = \sigma_0 M_{B0} f_b \sqrt{\frac{\pi a}{Q}} \quad (12)$$

where  $\sigma_0$  is the endurance limit,  $f_b$  is the applied bending stress,  $a$  is the minor axis of the assumed inherent quarter-elliptical defect,  $M_{B0}$  is the shape factor and  $Q$  is an elliptical integral (Broek, 1996).

#### Fatigue Crack Propagation Rate in Concrete

Wnuk (1971) derived a nonlinear differential equation governing the subcritical growth of a crack embedded in an elasto-plastic matrix up to the point of instabil-

ity. This work was extended to include time rate dependent effects Wnuk (1973). Ramsamooj (1994a) modified these theories to account for the different size of the inelastic zone, the effect of the minimum / maximum stress and the lower threshold stress intensity factor  $K_0$ .

The rate of crack propagation for high cycle fatigue (Ramsamooj, 1994a) is

$$\frac{dc}{dN} = \frac{K_{Ic}^2}{30 f_r^2} \left[ -\ln(1 - (R_f \Delta k)^2) - (R_f \Delta k)^2 \left(1 - \frac{2C}{f}\right) \right] \quad (13)$$

in which  $C = (d\psi/dt)_{t=0}$  = the initial rate of creep compliance of the concrete.

$$\Delta k = \frac{K_{I_{max}} - K_0}{K_{I_c}} \quad (14)$$

$$R = \frac{K_{I_{min}}}{K_{I_{max}}} \quad (15)$$

$$R_f = 1 - 0.2R - 0.8R^2 \quad (16)$$

in which  $K_{I_{min}}$  and  $K_{I_{max}}$  = the minimum and maximum SIFs, respectively.

The fatigue life  $N_f$  is defined arbitrarily as the number of cycles of load to cause the starter crack to grow to  $c_f = 1$  m, or

$$N_f = \int_{c_0}^{c_f} \frac{1}{\frac{K_{I_c}^2}{30f_r^2} \left[ -\ln(1 - (R_f \Delta k)^2) - (R_f \Delta k)^2 \left( 1 - \frac{2C}{f} \right) \right]} dc \quad (17)$$

Equation (17) was verified by Ramsamooj (1994a) using all of the major fatigue data on concrete beams published since 1920 by Lott and Kesler (1964), Murdoch and Kesler (1959), Raithby and Galloway (1974) and Ballinger (1970). It was validated for the 54 test sections of AASHO Road Tests (Ramsamooj, 1994b) which were subjected to 2 years of traffic (1958–1960) and open to traffic as part of the US interstate I-80 for the period 1960–1976 (Darter and Barenberg, 1977).

**Friction at Concrete/Subgrade Interface**

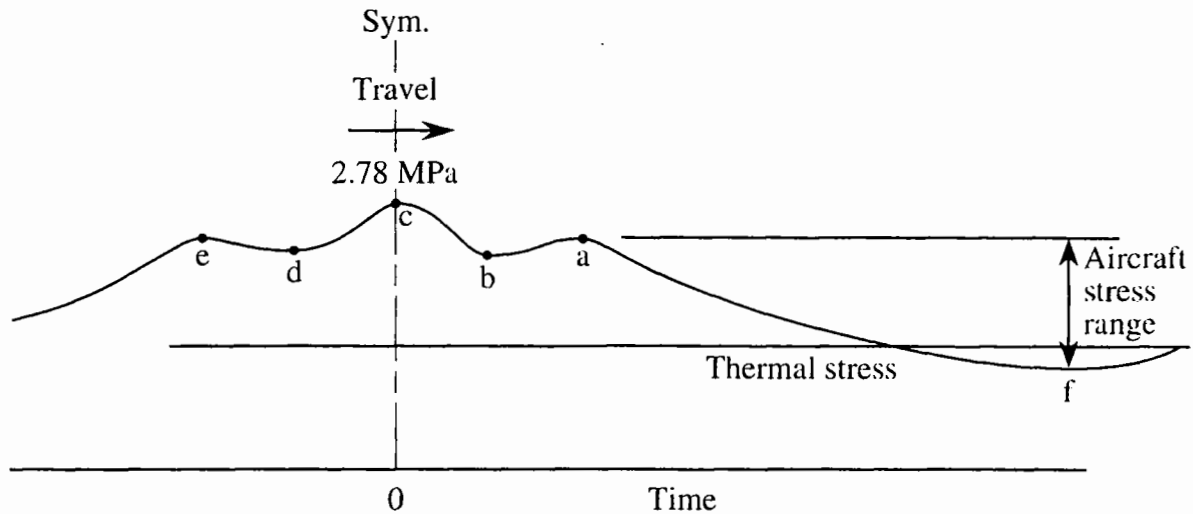
Any friction coefficient between the concrete and the subgrade can be used by placing a very thin layer (1.0 mm thick) of a low modulus material between the concrete and the subgrade. The angle of friction is  $\phi = \tan^{-1}(\tau_{rz}/\sigma_z)$  is obtained by changing the modulus of the interface layer iteratively.

**Temperature Curl Stress**

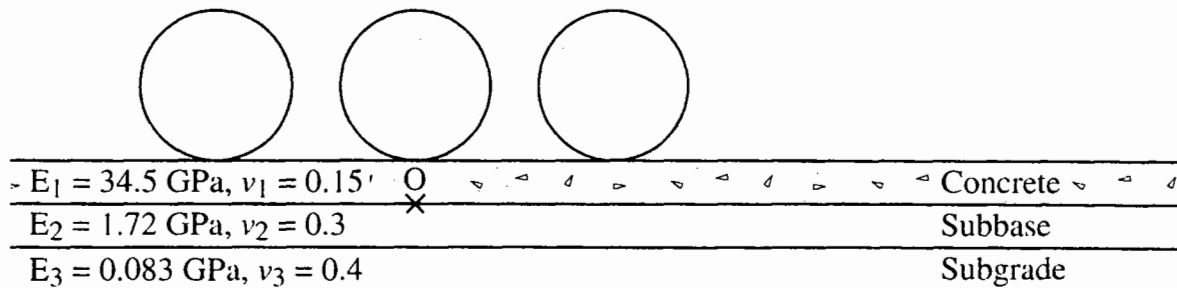
The EFM method is used to obtain the thermal curl stress (Ramsamooj, 1998). A brief summary is given here for the convenience of the reader. Consider a linear thermal gradient  $\theta$  with the top of the slab colder than the bottom so that the slab curls upward under the weight of the slab. Under the thermal curl alone the slab will be stress free because there is no constraint. The displacement at any point (x, y) measured from the origin at the corner is

$$w_T = \frac{\alpha\theta}{2}(x^2 + y^2) \quad (18)$$

in which  $\alpha$  = thermal coefficient of the PCC and  $\theta$  = thermal gradient.



(a) Stress Pulse



(b) Arrangement

FIGURE 3 Stress Pulse at O Generated by Boeing 777 Gear Loads

The curled slab is supported at the corners and the weight then exerts a stress that is determined as follows. Consider a continuous flat slab as shown in Figure 2 The deflection  $w$  is given by Timoshenko and Woinowsky-Kreiger (1959) as:

$$w = \frac{qb^4}{384D} \left( 1 - 4 \left( \frac{y}{b} \right)^2 \right)^2 + \frac{qa^3b}{2\pi^3D} \sum_{m=2,4,6}^{\infty} \left( \frac{(-1)^{m/2} \cos \frac{m\pi x}{a}}{m^3 \sinh \alpha_m \tanh \alpha_m} \right) \left( \frac{m\pi y}{a} \tanh \alpha_m \sinh \frac{m\pi y}{a} - (\alpha_m + \tanh \alpha_m) \cosh \frac{m\pi y}{a} \right) + A_o \quad (19)$$

where

$$A_o = -\frac{qa^3b}{2\pi^3D} \sum_{m=2,4,6}^{\infty} \frac{1}{m^3} \left( \alpha_m - \frac{\alpha_m + \tanh \alpha_m}{\tanh^2 \alpha_m} \right) \quad (20)$$

If frictionless joints are placed along the column centerlines, then a slab simply supported at the corners is obtained. The stresses are then determined by superposing those from the continuous flat slab on those generated by the cracks. The deflection consists of that of the continuous plate  $w_{cont}$  that caused solely by the joints  $w_j$  that caused by the subgrade reaction of the ground with a depth of embedment  $w_0$ , and that caused by the temperature curl  $w_T$ . The total deflection is

$$w = w_0 - w_T + w_{cont} + w_j \quad (21)$$

The radius  $R$  of the ground contact area is found from the condition that  $w = 0$ . The subgrade reaction is then  $q = kw$  ( $r < R$ ). Therefore

$$2\pi k \int_0^R wr \, dr = W \quad (22)$$

in which  $W$  = weight of the slab. The solution of Equations (21) and (22) gives the values of  $R$  and  $w_0$ . The maximum bending moment for the partially supported slab with a unit weight of  $q$  is then

$$M \max = 2kw \int_0^R r \, dr - 4qa^2 \quad (23)$$

### Stress Pulse of The Tridem Axle Gear Load, Boeing 777

The maximum gear load stresses occur at the longitudinal joint midway between the transverse joints. The maximum temperature gradient was assumed to be 0.022°C/mm. Computations using EFM show that the combined vehicular loading and thermal curl stress is approximately equal to that of the midslab joint bending stress without the thermal curl stress, so that when the thermal curl stress is included, the design is controlled by the midslab joint loading condition.

Fatigue cracks grow by blunting and resharping (Frost, 1965). In the loading portion of a stress pulse, a sharp crack in a tension field causes a large stress concentration at its tip, which leads to a blunt or rounded crack tip. Plastic deformation has occurred in a small region embedded in elastic surroundings. Dur-

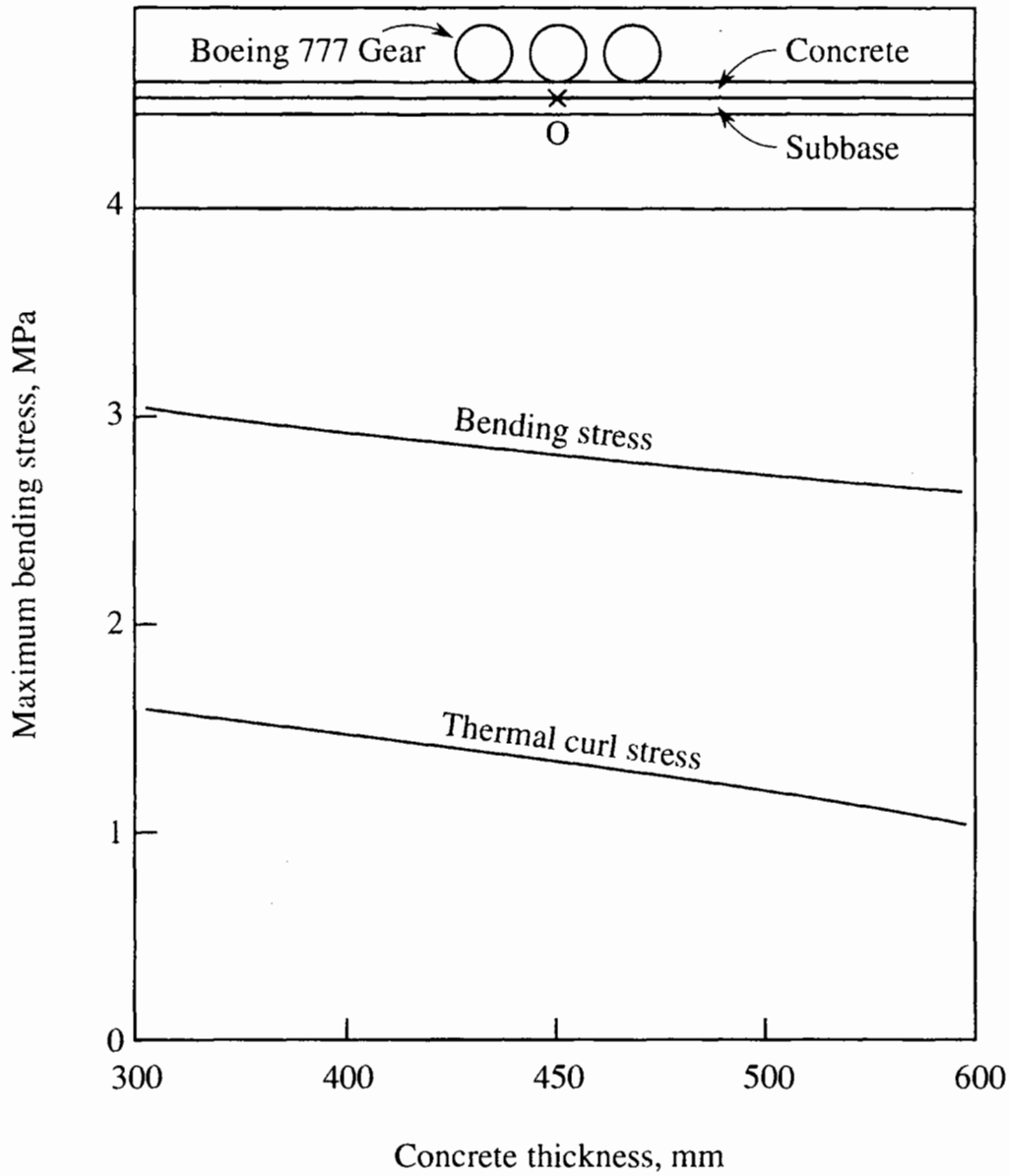


FIGURE 4 Thermal Curl Stress and Maximum Bending Stress at O, Gear Loads tangent to Longitudinal Joint

ing unloading the elastic region will exert compressive stresses on the plastically deformed region, which will close and resharpen the crack tip. This sequence of blunting and resharpening of the crack tip leads to fatigue crack propagation.

The tridem axle gear loads together with the thermal curl stress generate three pulses as shown in

Figure 3. If the load does not return to zero, there is a residual tensile stress, so that on reloading the crack tip opening does not begin to increase until a certain value of the SIF is reached. Each wheel load generates a pulse consisting of a tensile and a compressive peak. The combined effect of the superposition of the stresses caused by the gear load and thermal curl is

shown diagrammatically in Figure 3(a). The bottom of the first stress pulse at  $f$  is the algebraic sum of the temp curl stress and that caused by the compressive stress of the gear load. The minimum stress level halfway between the first and second wheels of the tridem axle plays an important role. For fatigue computations using Equation (17), the first pulse (Figure 3) has  $K_{min} = K_f$  and  $\Delta K = K_a - K_f$ , the second has  $K_{min} = K_b$  and  $\Delta K = K_c - K_b$  and the third pulse has  $K_{min} = K_d$  and  $\Delta K = K_e - K_d$ .

### Effect of Thermal Stresses caused by Temperature Gradient

The seasonal variation of the thermal gradient is obtained by extrapolating the results of the AASHO Road Test for a 439 mm thick concrete pavement (Darter and Barenberg, 1977). The daytime temperature gradient is assumed to vary according to

$$\theta = 0.0124 + 0.0096 \left( \sin \frac{\pi}{2} + \frac{2\pi N}{25000} \right) \quad (24)$$

where  $N$  is the number of applications of the tridem gear load, assumed to be applied at a constant rate of 25000 per year. The night-time temperature gradient is assumed to be constant at 0.011°C/mm. The thermal stress is assumed to be directly proportional to the temperature gradient and it is superposed on the stresses generated by the gear loads.

### Computer Program CONPAVE

Any lateral distribution of the axle loads across the pavement may be used. The distribution presently used is derived from PCA (Packard, 1973).

TABLE I Distribution of gear loads

Position measured from longitudinal edge, m	Percentage of gear load
-4.27 to 0.25	7.5
0.25 to 0.5	8.5
0.50 to 0.89	9.0
0.89 to 7.92	75.0

The *input* to CONPAVE is minimal and is as follows:

- NUMBER OF LAYERS
- YOUNG'S MODULUS AND POISSON'S RATIO FOR EACH LAYER
- THICKNESS OF EACH LAYER
- NUMBER OF RADII AND RADII
- NUMBER OF DEPTHS AND DEPTHS
- SPACING BETWEEN THE TRANSVERSE JOINTS
- MOD. OF RUPTURE, FRACTURE TOUGHNESS AND MAX. SIZE OF AGGREGATE
- SEASONAL MAXIMUM AND MINIMUM TEMP GRADIENT
- NO. AXLES/YR, FREQUENCY AND CREEP RATE OF CONCRETE

#### The Output

- THE DEFLECTION AND STRESSES AT THE MIDSLAB EDGE POSITION
- THE STRESSES ALONG THE MIDNORMAL TO THE LONGITUDINAL EDGE
- THE THERMAL CURL STRESSES
- THE CRACK LENGTH AS A FUNCTION OF THE NUMBER OF GEAR LOADS.

The following pavements were analyzed.

#### Concrete

Thickness, mm	=	406, 439, 508
Modulus of elasticity, GPa	=	34.5
Poisson's ratio	=	0.15
Compressive strength $f'_c$ , kPa	=	34480
Mod. of rupture, kPa	=	$58.6\sqrt{f'_c}$ *
Fracture toughness, $\text{kPa}\sqrt{m}$	=	1576
Endurance limit, kPa	=	$0.525f'_c$

#### Subbase - Cement treated

Thickness, mm	=	439
Modulus of elasticity, GPa	=	1.72
Poisson's ratio	=	0.3
Compressive strength $f'_c$ , kPa	=	4500

#### Clay Subgrade

Mod. of elasticity, MPa	=	82.7
-------------------------	---	------

Note:  $\sqrt{f'_c}$  in psi

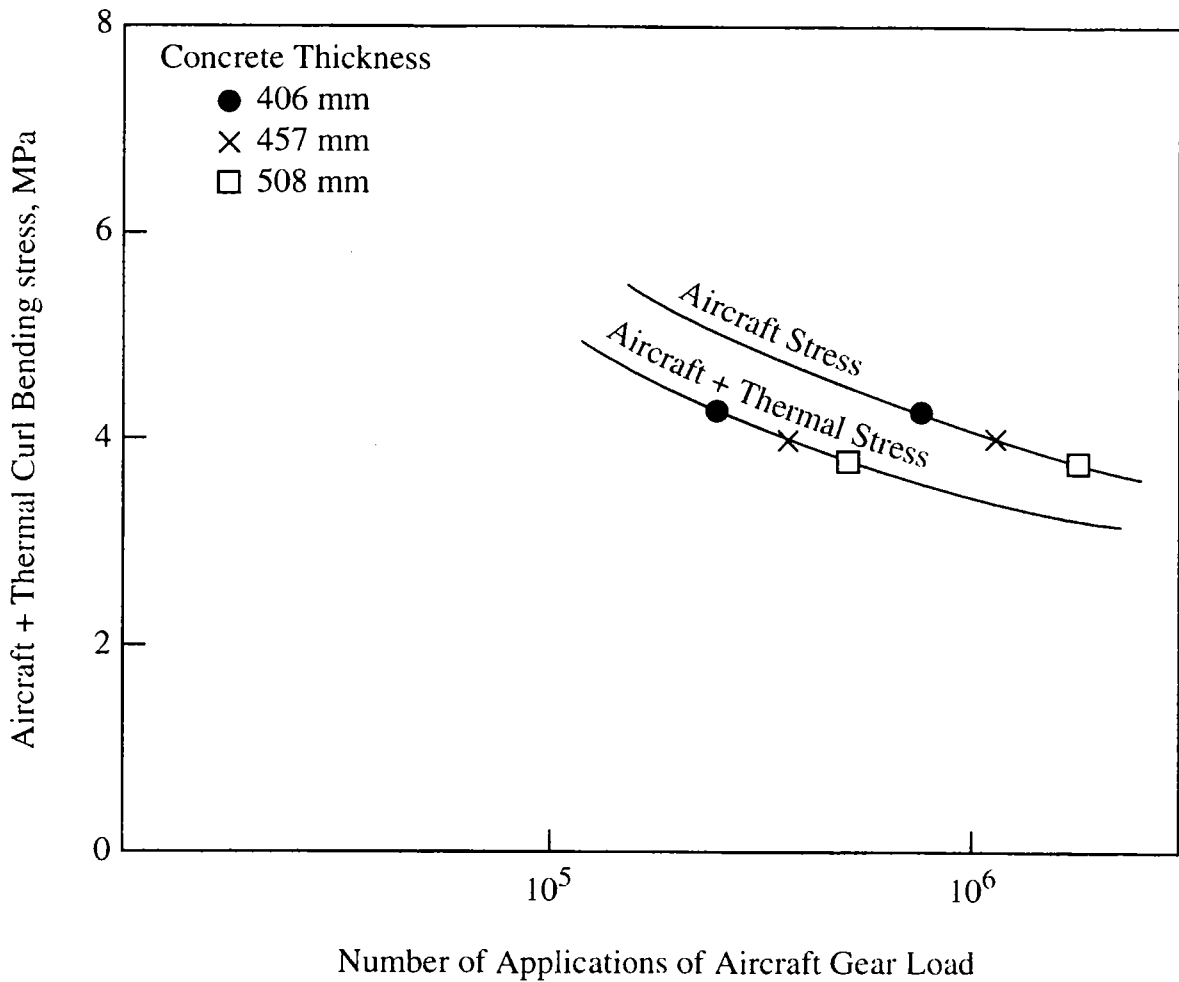


FIGURE 5 Fatigue Life versus Combined Aircraft and Thermal Curl Stress and from Aircraft Stress

The maximum stresses generated by the gear load and thermal curl for each pavement thickness are presented as functions of the concrete thickness in Figure 4. The fatigue life of the pavements is defined, arbitrarily, as the number of applications for the starter crack to grow to 1 m. The fatigue life computed by CONPAVE is presented graphically for the three pavements in Figure 5, under the combined stresses from the gear load and thermal curl, and from the gear loads alone. The effect of the thermal curl stress is seen to be much less severe than an increase in the aircraft gear load stress of the same amount.

The output of CONPAVE giving the number of applications of the aircraft for the combined gear loads and the thermal curl, is presented graphically in Figure 5. From this graph the thickness of the pavement for 500,000 applications in 20 years is selected as 457 mm., so that the final design consists of 457 mm of concrete on a 457 mm cement-treated subbase.

**CONCLUSIONS**

A rational design of a concrete runway has been presented. The effect of the thermal curl stress is merely

to increase the minimum level of stress resulting from aircraft and thermal loading. It is much less severe than an increase in the aircraft gear load stress of the same amount, but it is not negligible. The primary damage is caused by the cyclic stress range, so that it is very misleading to add the stresses caused by the gear loads and the thermal curl in any performance criteria.

The design is done by computer program called CONPAVE which requires less than fifteen seconds for the input data comprising the material properties, the loading and the temperature gradient. The output for the stresses and the fatigue life on a Pentium computer (233 MHz and 4 gigabytes of storage) is less than 4 minutes. The program automatically considers the lateral distribution of the traffic which may consist of a number of dual axle loads, single or tandem or tridem. The design is for Boeing 777 only, but a mixture of aircraft types poses no difficulty. The output gives the design stresses, the deflection and the fatigue life. In conclusion, the design captures the physical process of crack propagation using fundamental properties of the materials in accordance with the loading, boundary and environmental conditions.

### Acknowledgements

The author would like to thank the reviewers of this paper for their valuable suggestions, which led to significant improvement in the quality of the paper.

### References

- Ballinger (1970). Cumulative Fatigue damage Characteristics of Plain Concrete, SP 41-1, *Highway Research Board*, pp. 48-60.
- Broek, D. (1986). *Elementary Engineering Fracture Mechanics*, 4th ed., Martinus Nijhoff Publishers, 501 p.
- Chevron Oil Co. Ltd. (1978). Ten layer elastic stress distribution in flexible pavements.
- Clemmer, H. F. (1922). Fatigue of Concrete, *Proceedings ASTM*, Vol. 22, Pt II, 409-419.
- Darter, M. I. and Barenberg, E. J. (1977). Design of Zero-Maintenance Plain Jointed Concrete Pavements. *FHWA-RD-77-111*, 253 p.
- Darter, M. I., Hall, K. T. and Kuo, C. (1995). Support under Portland Cement Concrete Pavements. National Cooperative Research Program, *Transportation Research Board*.
- De-Chang, T., and J. Zhu. (1982). Crack Propagation under Combined Stresses in Three-dimensional Medium. *Engineering Fracture Mechanics*, Vol. 16, No. 1, pp. 5-7.
- Folias, E. S. (1970). On a Plate supported on an Elastic Foundation and containing a finite Crack, *Int. Journal of Fracture Mechanics*, 6:3, 257-263.
- Frost, N. E. (1965). The Growth of Fatigue Cracks, *Proc. 1st Int. Conf. on Fracture*, Vol. 3, 1433-1450, Sendai, Japan.
- Grandt, A. F. Jr. and G. M. Sinclair (1972). Stress Intensity factors for Surface Cracks In Bending, *Stress Analysis and Growth of Cracks, Proc. of 1971 Nat. Sym. on Fracture Mechanics, Pt. 1, ASTP 513*, 37-58.
- Huang, Y. H. (1953). *Pavement Analysis and Design*, Prentice Hall, 805pp.
- Kesler, C. E. (1953). Effect of Speed of Testing on Flexural Fatigue of Plain Concrete, *Proc. of The Highway Research Board*, Vol. 32, pp. 251-258.
- Lott, G. L. and Kesler, C. E. (1964). *Crack Propagation in Plain Concrete*, TAM Report 622, Department of Theoretical and Applied Mechanics, University of Illinois, Urbana, Ill.
- Murdock, J. W. and Kesler, C. E. (1959). Effect of the Range of Stress on Fatigue Strength of Plain Concrete Beams, *Proceedings, of The American Concrete Institute*, Vol. 55, pp. 221-231.
- Nordby, G.M. (1958) Fatigue of Concrete - A Review of Research, *ACI Committee 215*, 191-219.
- Ouchterlony, F. (1983). Fracture Toughness Testing, *Rock Fracture Mechanics*, ed. Rossmannith, New York, 69-150.
- Packard, R. G., (1973). *Design of Concrete Pavements*, Portland Cement Association, 61 p.
- Petroski, H. J. and J. D. Achenbach (1978). Computation of the Weight Function from a Stress Intensity Factor. *Engineering Fracture Mechanics*, Vol. 10, 257-266.
- Raithby, K. W. and Galloway, J. W. (1974). Effect of Moisture Condition, Age and Rate of loading on Fatigue of Plain Concrete, SP 41-2, *American Concrete Institute*, pp. 15-33.
- Ramsamooj, D. V. (1994a). Prediction of Fatigue Life of Plain Concrete Beams from Fracture Tests. *ASTM Journal of Materials & Testing*, pp. 183.
- Ramsamooj, D. V. (1994b). Prediction of Fatigue Cracking of Rigid Pavements. *Third International Workshop on the Design and Evaluation of Concrete Pavements. CROW, Austria*, pp. 401-409.
- Ramsamooj, D. V. (1998). Temperature curl stresses in pavements Fourth Int. Workshop on design theories and their verification of concrete slabs for pavements and railroads CROW, Lisbon, Portugal.
- Ramsamooj, D. V., G. S. Lin and J. Ramadan (1998). Stresses caused by Joints and Cracks in Highway and Airport Pavements with Overlays. *Engineering Fracture Mechanics*, Vol. 44, No. 4, pp. 609-626.
- Ramsamooj, D. V. (1999). Stresses on Jointed Rigid Pavements. *Engineering Fracture Mechanics*, Vol. 125, No. 2, pp. 101-107.
- Sih, G. and H. Liebowitz (1968). Mathematical Theories of brittle fracture. *Fracture. An Advanced Treatise*. Vol. II, pp. 1-190.
- Timoshenko, S. and Woinowsky-Kreiger, S. (1959). *Theory of Plates and Shells*, McGraw Hill, Book Co., N.Y.
- Westergaard, H.M. (1948). New Formulas for Stresses in Concrete Pavements of Airfields. *Transactions ASCE*, Vol. 113, 425-444.
- Wnuk, M. P. (1971). Subcritical Growth of Fracture, *International Journal of Fracture Mechanics*, 7, Vol. 4, pp 383-486.
- Wnuk, M.P., (1973). Prior to Failure Extension of Flaws under Monotonic and Pulsating Loadings, *Engineering Fracture Mechanics*, Vol. 5 179-196.

## Appendix Notation

The following symbols are used in this paper:

$a, c$	semi-elliptical minor and major axis of crack
$a/c$	shape factor
$d$	maximum size of aggregate
$f$	frequency of loading
$f_b$	bending stress in the uncracked beam;
$E$	modulus of concrete
$E_s$	modulus of the subgrade
$G, G_C$	strain energy release rate, and its critical value
$H$	thickness of the concrete slab
$k$	coefficient of subgrade reaction
$K_I, K_{IC}$	SIF in the opening mode and its critical value
$K_o$	value of $K_I$ at the endurance limit
$K_{max}$	maximum value of $K_I$ ,
$N$	number of cycles of load
$R$	ratio of min. and max. stress during cyclic loading
$\sigma_t = f_r$	yield stress in flexural tension or the modulus of rupture
$\nu$	Poisson's ratio.
$\lambda$	$\sqrt[4]{\frac{k}{D}}$ = inverse characteristic stiffness,
$c_0$	inherent crack length